J Sci Comput (2015) 63:49–77
DOI 10.1007/s10915-014-9886-1

A Spectral Study on the Dissipation and Dispersion of the WENO Schemes

Feilin Jia · Zhen Gao · Wai Sun Don

Received: 26 November 2013 / Revised: 17 April 2014 / Accepted: 25 June 2014 /
Published online: 9 July 2014

Abstract The dissipation and dispersion (spectral) properties of the nonlinear fifth order classical weighted essentially non-oscillatory finite difference scheme (WENO-JS5) and its improved version (WENO-Z5) using the approximate dispersion relation (ADR) (Pirozzoli in J Comput Phys 219:489–497, 2006) and the nonlinear spectral analysis (NSA) (Fauconnier et al. in J Comput Phys 228(6):1830–1861, 2009) are studied. Unlike the previous studies, the influences of the sensitivity parameter in the definition of the WENO nonlinear weights are also included for completeness. The fifth order upwinded central linear scheme (UW5) serves as the reference and benchmark for the purpose of comparison. The spectral properties of the WENO differentiation operator is well predicted theoretically by the ADR and validated numerically by the simulations of the WENO schemes in solving the scalar linear advection equation. In a long time simulation with an initial broadband wave, the WENO schemes generate spurious high modes with amplitude and spread of wavenumbers depend on the value of the sensitivity parameter. The NSA is applied to investigate the statistical nonlinear behavior, due to the nonlinear stencils adaptation of the WENO schemes, with a large set of initial conditions consisting of synthetic scalar fields with a prescribed energy spectrum and random phases. The statistics indicate that there is a small probability of an existence of a mild anti-dissipation in the low wavenumber range regardless of the size of the sensitivity parameter. Numerical examples demonstrate that the WENO-Z5 scheme is not only less dissipative and dispersive but also less sensitive to random phases than the WENO-JS5 scheme. Furthermore, a sensitivity parameter adaptive technique, in which its value depends

F. Jia
School of Aerospace Engineering, Beijing Institute of Technology, Beijing, China
e-mail: jiafeilin1990@gmail.com

Z. Gao (✉) · W. S. Don
School of Mathematical Sciences, Ocean University of China, Qingdao, China
e-mail: zhengao@ouc.edu.cn

W. S. Don
Division of Applied Mathematics, Brown University, Providence, RI 20912, USA
e-mail: wsdon@dam.brown.edu

on the local smoothness of the solution at a given spatial location and time, is introduced for solving a linear advection problem with a discontinuous initial condition. The preliminary result shows that the solution computed by the sensitivity parameter adaptive WENO-Z5 scheme agrees well with those computed by the WENO-Z5 scheme and the UW5 scheme in regions containing discontinuities and smooth solutions, respectively.

Keywords Weighted essentially non-oscillatory · WENO-JS · WENO-Z · Approximate dispersion relation · Nonlinear spectral analysis · Modified wavenumber

Mathematics Subject Classification 65P30 · 77Axx

1 Introduction

Weighted Essentially Non-Oscillation (WENO) conservative finite difference schemes on an equidistant stencil as a class of high order/high resolution nonlinear shock-capturing schemes (nonlinear schemes) for solutions of hyperbolic conservation laws in the presence of shocks and small scale structures were developed (for details and history of WENO schemes, see [14] and references contained therein). The use of a dynamic set of substencils where a nonlinear convex combination of lower order (local) polynomials *adapts* through the use of nonlinear weights either to form a polynomial of order $O(\Delta x^{2r-1})$ at a smooth stencil, or to form a polynomial of lower order $O(\Delta x^r)$ in a non-smooth stencil. The smoothness of a given substencil is measured by the smoothness indicators $\{\beta_k\}_{k=0}^{r-1}$ that measure the normalized Sobolev norm of all the derivatives of each local polynomial. The nonlinear weights ω_k, such as the classical weights given in the classical WENO-JS scheme [8] and the optimal weights given in the improved WENO-Z scheme [2,3], used in the formation of the convex combination of the local polynomials at the cell interface, have been used extensively. It has been numerically demonstrated that the WENO finite difference scheme based on the improved WENO-Z scheme is less dissipative and has a higher resolution power than the classical WENO-JS scheme for a larger class of problems. A detailed analysis of the nonlinear schemes has been difficult as the behavior of the schemes depends on the solution and vice versa, and a couple user tunable parameters, for example, the sensitivity parameter (ϵ) and the power parameter (p) that appear in the formulation of the nonlinear weights.

Recently, the dissipation and dispersion (spectral) properties and the influence of non-linearity of, such as the fifth order WENO-JS5 scheme and the TVD schemes based on the use of flux limiters [11], the nonlinear schemes on the solution of a scalar *linear* advection problem have been studied in [6,7,9,13]. Ladeinde et al. [9] focused on the comparative differential representation of the spectral distribution of turbulence energy as computed by several nonlinear schemes. Pirozzoli et al. [13] proposed the approximate dispersion relation (ADR) to analyze and to predict theoretically the performance of the WENO-JS5 scheme in the Fourier (wavenumber) space. The individual spectral properties of a simple sinusoidal wave with a few chosen wavenumbers have been independently analyzed using the results obtained from solving the *linear* advection equation by a *nonlinear* scheme. It was shown that the modified wavenumbers predicted by the ADR and computed by the WENO-JS5 scheme can closely track the dissipation and dispersion of each wavenumber. However, the ADR does not take into account of the nonlinear interactions between waves with different wavenumbers in a long time simulation. Fauconnier et al. [5–7] proposed a nonlinear spectral analysis (NSA) to study the statistical behavior of the full spectrum of modified wavenumbers of the WENO-JS5 scheme, the TVD scheme, and the Nonlinear Dynamic Finite Difference

(DFD) scheme, for large samples of synthetic scalar field with a prescribed energy spectrum and random phases, which serves as an initial condition of the advection equation. However, the ADR and NSA have not been extended to examine the spectral properties of the improved WENO-Z scheme, and there is a lack of study regarding the influences of the sensitivity parameter ϵ found in the definition of the WENO nonlinear weights on the spectral properties of the WENO-JS and WENO-Z schemes (referred collectively as the WENO schemes).

In this work, we investigate the spectral properties of the fifth order WENO *nonlinear* schemes using both the ADR and NSA and compare their results with those obtained from an optimal fifth order central upwinded finite difference *linear* scheme (UW5), which also serves as the benchmark for comparison purpose. Unlike the previous studies, the presence of the ϵ and the influences it has on the spectral properties of the WENO schemes are also taken into consideration. We first perform the ADR on sinusoidal waves with four representative wavenumbers. We show that the ADR has the ability to predict accurately the spectral properties of the WENO schemes, as validated by analyzing the solution of the linear advection equation computed by the WENO schemes for a very short time in the Fourier space. The spectral properties favor the WENO-Z5 scheme over the WENO-JS5 scheme over a full resolvable spectrum. A comparison with the UW5 scheme is also conducted with an initial broadband wave. It has been shown that spurious high modes can be generated by the nonlinearity of the WENO schemes, which is absent in the linear UW5 scheme. The amplitude and spread of the spurious high modes are weakly affected by the value of ϵ.

In the ADR, all resolvable wavenumbers are treated as equally important, which is not likely to be the case in a smooth flow. The NSA is used to further analyze the spectral properties of the WENO schemes statistically. This allows one to investigate the long time impact of the nonlinearity of the WENO schemes on the energy spectrum of a more realistic smooth flow containing many small scale structures, for example, isotropic turbulence. Here, the ϵ also plays an important role in determining the error in the energy spectrum of the field and the energy spectrum of the error of the field. Again, the spectral properties favor the WENO-Z scheme over the WENO-JS scheme for linear problems with many small scale structures. We also show that there is a tiny probability (two standard deviations from the mean) of the presence of anti-dissipation in a low wavenumber range, in which the amplitude of a wave is being amplified slightly instead of being reduced strongly in the Fourier space.

Ultimately, the WENO schemes are designed for solving problems with solution containing both discontinuous and smooth regions. In the spectral analysis of the WENO schemes, the sensitivity parameter ϵ plays a relatively minor role. The larger the ϵ is, the smaller the dissipation and dispersion errors, the spurious high frequency noises, and the influence of nonlinearity would become. However, for a discontinuous solution, the ϵ must be sufficiently small in order to capturing the shocks in an essentially non-oscillatory manner. These two competing requirements exist simultaneously in the solution of nonlinear hyperbolic conservation laws. As an interesting consequence of the present study, we show a preliminary result of adapting the value of the sensitivity parameter $\epsilon(x, t)$ spatially and temporally based on the local smoothness of the solution. The solution of an advection of an initial square wave shows that the solution behaves like the UW5 scheme in the smooth regions and the WENO schemes in the regions containing discontinuities. By designing a good technique in adapting the $\epsilon(x, t)$, this ϵ-adaptive WENO scheme approach holds a promise that one can obtain the desirable spectral properties of an optimal order linear scheme while capturing discontinuities essentially non-oscillatory by the WENO schemes.

The paper is organized as follows. In Sect. 2, a brief introduction to the classical WENO-JS5 scheme, the improved WENO-Z5 scheme, and the central upwinded UW5 scheme for solving hyperbolic conservation laws are given. In Sects. 3 and 4, we briefly introduce the

ADR and NSA, respectively, on how to analyze the spectral properties of a numerical scheme. The spectral properties of the WENO-JS5 and WENO-Z5 schemes using the ADR and NSA are also shown with various sensitivity parameters. In Sect. 5, an ϵ-adaptive WENO scheme is proposed and a preliminary result is shown. Conclusion and future work are discussed in Sect. 6.

2 Numerical Schemes

In this section, we briefly describe the fifth order weighted essentially non-oscillatory finite difference nonlinear scheme (WENO) and the fifth order upwinded central finite difference linear scheme (UW5) for solving a one dimensional scalar hyperbolic conservation laws,

$$\frac{\partial u}{\partial t} + \frac{\partial f(u)}{\partial x} = 0. \tag{1}$$

2.1 Nonlinear Weighted Essentially Non-oscillation Schemes

Consider a uniform grid defined by the points $x_i = i\Delta x, i = 0, \ldots, N$, which are called cell centers, with cell boundaries given by $x_{i+\frac{1}{2}} = x_i + \frac{\Delta x}{2}$, where Δx is the uniform grid spacing (see Fig. 1). By integrating (1) over each cell, one has

$$\frac{du_i(t)}{dt} = -\left.\frac{\partial f}{\partial x}\right|_{x=x_i} \approx -\frac{1}{\Delta x}\left(h_{i+\frac{1}{2}} - h_{i-\frac{1}{2}}\right) + O(\Delta x^5), \quad i = 0, \ldots, N, \tag{2}$$

where $u_i(t)$ is a numerical approximation to the cell-averaged value $u(x_i, t)$ and $h_{i\pm\frac{1}{2}} = h(x_{i\pm\frac{1}{2}})$ is a high order polynomial interpolation based on the known cell-averaged values $f_j = f(x_j), j = i-2, \ldots, i+2$ and evaluated at the cell boundary $x = x_{i\pm\frac{1}{2}}$. It is easy to see that the numerical flux function $h(x)$ is related to the flux function $f(x)$ implicitly as

$$f(x) = \frac{1}{\Delta x}\int_{x-\frac{\Delta x}{2}}^{x+\frac{\Delta x}{2}} h(\xi)d\xi. \tag{3}$$

Here, we describe the nonlinear WENO reconstruction procedure, which is the heart of any WENO scheme. The procedure uses five points global stencil $S^5 = \cup_{k=0}^{2} S_k$ which contains three substencils $S_k = \{x_{i+k+j-2}, j = 0, 1, 2\}$ for a given cell center x_i. The numerical flux $h_{i\pm\frac{1}{2}}$ is approximated by a fifth degree polynomial $\hat{f}(x_{i\pm\frac{1}{2}})$, which is a convex combination of three second degree local polynomials $\hat{f}^k(x)$ in each S_k at $x_{i\pm\frac{1}{2}}$, as

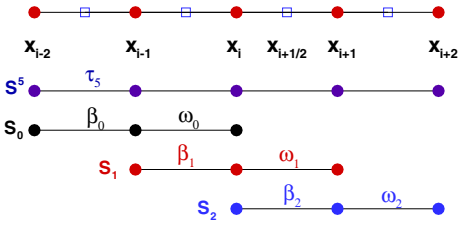

Fig. 1 The computational uniformly spaced grid x_i and the 5-points stencil S^5, composed of three 3-points substencils $\{S_0, S_1, S_2\}$, used for the fifth-order WENO reconstruction step

$$\hat{f}_{i\pm\frac{1}{2}} = \sum_{k=0}^{2} \omega_k^{\pm} \hat{f}^k(x_{i\pm\frac{1}{2}}) \approx h_{i\pm\frac{1}{2}} + O(\Delta x^5), \tag{4}$$

where

$$\hat{f}^k(x_{i+\frac{1}{2}}) = \hat{f}^k_{i+\frac{1}{2}} = \sum_{j=0}^{2} c_{kj} f_{i-k+j}, \quad i = 0, \ldots, N, \tag{5}$$

$\hat{f}^k_{i-\frac{1}{2}}$ can be found by symmetry. The c_{kj} are the Lagrangian interpolation coefficients (see [8]) and ω_k are the nonlinear weights, which will be described below.

The modified Sobolev norm of the interpolation polynomial $\hat{f}^k(x)$ defines the local smoothness indicator β_k, which measures the local smoothness of $\hat{f}^k(x)$ in the substencil S_k at x_i, as

$$\beta_k = \sum_{l=1}^{2} \Delta x^{2l-1} \int_{x_{i-\frac{1}{2}}}^{x_{i+\frac{1}{2}}} \left(\frac{d^l}{dx^l} \hat{f}^k(x) \right)^2 dx. \tag{6}$$

2.1.1 Classical WENO Scheme (WENO-JS5)

In the fifth order classical WENO-JS scheme [1,8], the nonlinear weights ω_k are defined as

$$\alpha_k = \frac{d_k}{(\beta_k + \epsilon)^p}, \quad \omega_k = \frac{\alpha_k}{\sum_{l=0}^{2} \alpha_l}, \qquad k = 0, 1, 2. \tag{7}$$

The coefficients $\left\{ d_0 = \frac{3}{10},\ d_1 = \frac{3}{5},\ d_2 = \frac{1}{10} \right\}$ are the ideal weights that, when the solution is sufficiently smooth, one has $\{\omega_k \approx d_k\}$ and the WENO scheme *essentially* becomes the optimal fifth order central upwind scheme (UW5) (see Sect. 2.2).

2.1.2 Improved WENO Scheme (WENO-Z5)

In the fifth order improved WENO-Z5 scheme [2,3], the nonlinear weights ω_k^Z are defined as

$$\alpha_k^Z = d_k \left(1 + \left(\frac{\tau_5}{\beta_k + \epsilon} \right)^p \right), \quad \omega_k^Z = \frac{\alpha_k^Z}{\sum_{l=0}^{2} \alpha_l^Z}, \quad k = 0, 1, 2, \tag{8}$$

with the optimal order smoothness indicator $\tau_5 = |\beta_2 - \beta_0|$, which has a leading truncation error of order $O(\Delta x^5)$ by the Taylor series expansion. In contrary, the leading truncation error of β_k are of order $O(\Delta x^2)$. Strictly speaking, the leading truncation error estimates of β_k and τ_5 are only valid if $f'(x_i) \neq 0$.

Remark 1 In general, the power parameter $p = 2$ is used to enhance the relative ratio between the smoothness indicators β_k and the sensitivity parameter $\varepsilon > 0$ (Typically $10^{-6} - 10^{-16}$ is used to avoid a division by zero in the nonlinear weights formulation).

Remark 2 Theoretically speaking, the nonlinearity of a nonlinear scheme depends weakly and continuously on the ϵ regardless of what its value is. As shown later, even for a simple linear equation such as the linear advection equation, the nonlinearity of a nonlinear scheme could generate spurious high modes which might pollute the flow field, and for a nonlinear equation, if not removed, might generate spurious solution in the full wavenumber spectrum due to the nonlinear interaction among low and high modes.

Remark 3 In [2,3], the improved performance of the WENO-Z5 scheme over the WENO-JS5 scheme has been demonstrated conclusively in computing a higher resolution solution when solving hyperbolic conservation laws for both smooth and discontinuous solutions. In [4], the WENO-Z5 scheme has been shown, in comparison to the WENO-JS5 scheme, to allow a more flexible choice on the ϵ as a function of grid spacing Δx that will guarantee the formal order of convergence of the nonlinear scheme regardless of the critical points while maintaining the essentially non-oscillatory nature of the shock-capturing scheme. Readers are referred to [2–4] for more details.

2.2 Linear Upwinded Central Scheme (UW5)

The numerical flux of the fifth order upwinded central finite difference linear scheme (UW5) shares the same global stencil S^5 as the fifth order nonlinear WENO schemes. As a matter of fact, for a smooth function, the UW5 scheme is theoretically equivalence to the *optimal* fifth order WENO schemes, that is, the nonlinear weights are equal to the ideal weights ($\omega_k = \omega_k^Z = d_k$). Furthermore, the numerical flux at the cell-boundary $h_{i+\frac{1}{2}}$ in terms of cell-center values $\{f_{i-2}, \ldots, f_{i+2}\}$ simply becomes

$$h_{i+\frac{1}{2}} = \frac{1}{36}\left(2f_{i-2} - 13f_{i-1} + 47f_i + 27f_{i+1} - 3f_{i+2}\right). \tag{9}$$

The derivative of $f(x)$, $\frac{\partial f}{\partial x}$, follows by (2) and is of order $O(\Delta x^5)$.

Remark 4 For a smooth solution, the nonlinear WENO schemes theoretically become the optimal linear UW5 scheme, which has the optimal spectral properties of the underlying nonlinear scheme. That is, the spectral properties of the WENO scheme approach those of the UW5 scheme in the limit of increasing smoothness of the reconstructed flux function. Hence, the spectral properties of the UW5 scheme is used as a benchmark and reference in the study that follows.

2.3 Notations

In the following discussions, we will adopt the following notations for clarity and ease of reading.

Notation 1 We shall refer collectively both the WENO-JS and WENO-Z schemes as the WENO schemes or the nonlinear schemes, and the UW scheme as the linear scheme, when it is clear in the context of the discussion.

Notation 2 We will append the power of the sensitivity parameter $\varepsilon = 10^{-n}$ to the name of the WENO schemes, when necessary, as in WENO-JS5`en` or WENO-Z5`en`, in order to denote a fifth order WENO scheme with a different ε under investigation. For example, `WENO-JS5e6` denotes the fifth order WENO-JS scheme with $\varepsilon = 10^{-6}$. In the case when ε is chosen adaptively, the notation `eXX` will be used instead.

Notation 3 Since only the fifth order schemes are used in this study, we shall omit the number `5` in the notation in the text unless it is deemed necessary for clarity purpose.

3 Approximate Dispersion Relation

In this section, we briefly describe the approximate dispersion relation (ADR) [13] that is used to predict theoretically the dissipation and dispersion (spectral) properties of a general

numerical scheme. The technique evolves a single Fourier mode in a periodical domain by a *linear* advection equation with a constant speed in a limit with $\Delta t \to 0$. The solution is then analyzed in the Fourier space to obtain the spectral properties of the scheme.

We consider the linear advection equation with flux $f(u) = u$ in (1),

$$\frac{\partial u}{\partial t} + \frac{\partial u}{\partial x} = 0, \quad |x| < \infty, t > 0, \tag{10}$$

and an initial condition consisting of a single sinusoidal wave with wavenumber κ,

$$u(x, 0) = e^{i\kappa x}. \tag{11}$$

The semi-discrete approximation of (10) at grid points $x_j = j\Delta x$, $j = 0, \ldots, N$ in a 2π-periodical domain, where N is the number of grid points and $\Delta x = 2\pi/N$ is the uniform grid spacing, is

$$\frac{\partial v_j}{\partial t} + \frac{\partial v_j}{\partial x} = 0, \quad x \in [0, 2\pi), \quad t > 0, \tag{12}$$

with the discretized initial condition

$$v_j(0) = e^{ij\kappa\Delta x}, \tag{13}$$

where $v_j(t) \approx u(x_j, t)$, $|\kappa| \leq N/2$ is the discrete wavenumber and $|\omega| = |\kappa\Delta x| \leq \pi$ is the discrete angular wavenumber [10].

The spatial derivative of $v(x, t)$ at x_j, $\frac{\partial v_j}{\partial x}$, is discretized by a standard *linear* finite-difference scheme as

$$\frac{\partial v_j}{\partial x} = \frac{1}{\Delta x} \sum_{l=-q}^{r} \alpha_l v_{j+l} \approx \left.\frac{\partial u}{\partial x}\right|_{x=x_j}, \tag{14}$$

where α_l are the finite difference weights.

It follows from [15] that (12) has an exact solution

$$v_j(t) = \hat{v}(t) e^{ij\omega}, \tag{15}$$

where the complex amplitude of the solution at time t, $\hat{v}(t)$, is given by

$$\hat{v}(t) = e^{-i(t/\Delta x)W(\omega)}, \tag{16}$$

with a modified wavenumber $W(\omega) = -i \sum_{l=-q}^{r} \alpha_l e^{il\omega}$.

According to [13], no analytical formula of dissipation and dispersion relationships can be obtained for a nonlinear scheme due to its nonlinear switching (e.g. TVD schemes) or adaptation (e.g. WENO schemes) of substencils based on the underlying smoothness of the solution. Instead, one can define the ADR by considering a sinusoidal initial condition with an assigned wavenumber ω, that is, $v_j(0) = e^{ij\omega}$, and then advancing the solution forward to the final time $t = \Delta t \to 0$, $v_j(\Delta t)$, in order to minimize the time discretization error. The discrete Fourier transform of the computed solution $v_j(\Delta t)$ yields the Fourier spectrum of the solution associated with the given wavenumber ω, $\hat{v}(\omega; \Delta t)$.

From (16), one can define a modified wavenumber

$$W(\omega) = \frac{i}{\sigma} \ln\left(\hat{v}(\omega; \Delta t)\right), \tag{17}$$

where $\sigma = \Delta t/\Delta x \ll 1$, generated by a nonlinear scheme in solving (10) at time Δt.

It is known that the resolvable wavenumber ω on a uniformly spaced grid with N grid points satisfies the condition $|\omega| = |\kappa \Delta x| \leq \pi, |\kappa| \leq N/2$. In practice, the above procedure is repeated for different resolvable wavenumber ω to obtain its corresponding modified wavenumber $W(\omega)$. This process enables one to construct the ADR that accounts for the leading order of the nonlinear effects embodied in the nonlinear schemes. We refer to [13] for details. By examining the real and imaginary parts of the modified wavenumber $W(\omega)$, one can gain important insights on the spectral properties of the underlining nonlinear scheme. It allows one to quantify, in terms of dissipation and dispersion, in some fashion, how well a nonlinear scheme would perform in an idealized situation (solving a linear wave equation with an initial condition consisting of only a single sinusoidal wave with a fixed wavenumber to a very short final time) as compared to a linear scheme.

Remark 5 Due to the symmetry and anti-symmetry of the modified wavenumbers, one has $W(-\omega) = \bar{W}(\omega)$ and $W(-\omega) = -\bar{W}(\omega)$, respectively, where $\bar{W}$ denotes the complex conjugate of W. Hence, only the positive half of wavenumber spectra $\omega \geq 0$ are used in following discussions and figures.

3.1 ADR for an Initial Single Mode Sinusoidal Wave

First, we show the performance of the ADR and compare them with solution computed by the UW scheme, the WENO-JS scheme, and the WENO-Z scheme in solving a linear advection problem with an initial condition consisting of a single mode sinusoidal wave (with wavenumber κ) in a 2π periodical domain, that is, $v(x,t) = e^{i\kappa x}$. Since the solution is smooth, the sensitivity parameter ϵ plays essentially no role in this case. Here we use $\epsilon = 10^{-16}$.

As shown in Fig. 2, the dispersion (real part of $W(\omega)$) and the dissipation (imaginary part of $W(\omega)$) of the UW scheme and the WENO schemes agree very well with those given in [13]. We observe that, due to the nonlinear stencils adaptation effect, the spectral properties of the WENO schemes are different from those of the UW scheme. The WENO schemes behave similarly until $|\omega| \leq 1$ for dispersion and $|\omega| \leq 0.75$ for dissipation. At higher wavenumbers, the WENO-Z scheme is less dispersive for $|\omega| \leq 1.5$ and less dissipative for all wavenumbers ω than the WENO-JS scheme. The UW scheme has the least dissipation and dispersion errors among the three schemes.

To demonstrate the spectral properties of the WENO schemes, the temporal evolution of the amplitude of four Fourier modes from low to high wavenumbers $\omega = \pi/8, \pi/4, 3\pi/8$ and $\pi/2$ are shown in Fig. 3. The solution's amplitude predicted by the ADR is

$$|\hat{v}(\omega, t)| = |\hat{v}_0(\omega)| e^{(t/\Delta x)\mathrm{Imag}[W(\omega)]}, \tag{18}$$

where $W(\omega)$ is computed by (17) for the WENO schemes. The results show a very good agreement between the theoretical prediction (solid lines) by the ADR and the numerical prediction (symbols) as computed by the WENO schemes, which also agree very well with those given in [13].

Figure 4 shows how well the temporal evolution of the amplitudes of four individual Fourier modes with wavenumbers $\omega = \pi/8, \pi/4, 3\pi/8, \pi/2$ as computed by the WENO schemes and the UW scheme. All three schemes show the decay of the amplitude over time due to the dissipative nature of the schemes. At the low wavenumber $\omega = \pi/8$, all three schemes (black solid line and two triangle symbols) behave in a very similar fashion. At the medium range wavenumbers $\omega = \pi/4$ and $\omega = 3\pi/8$, the WENO-Z scheme (blue square and circle symbols) and the UW scheme (blue and red solid lines) decay

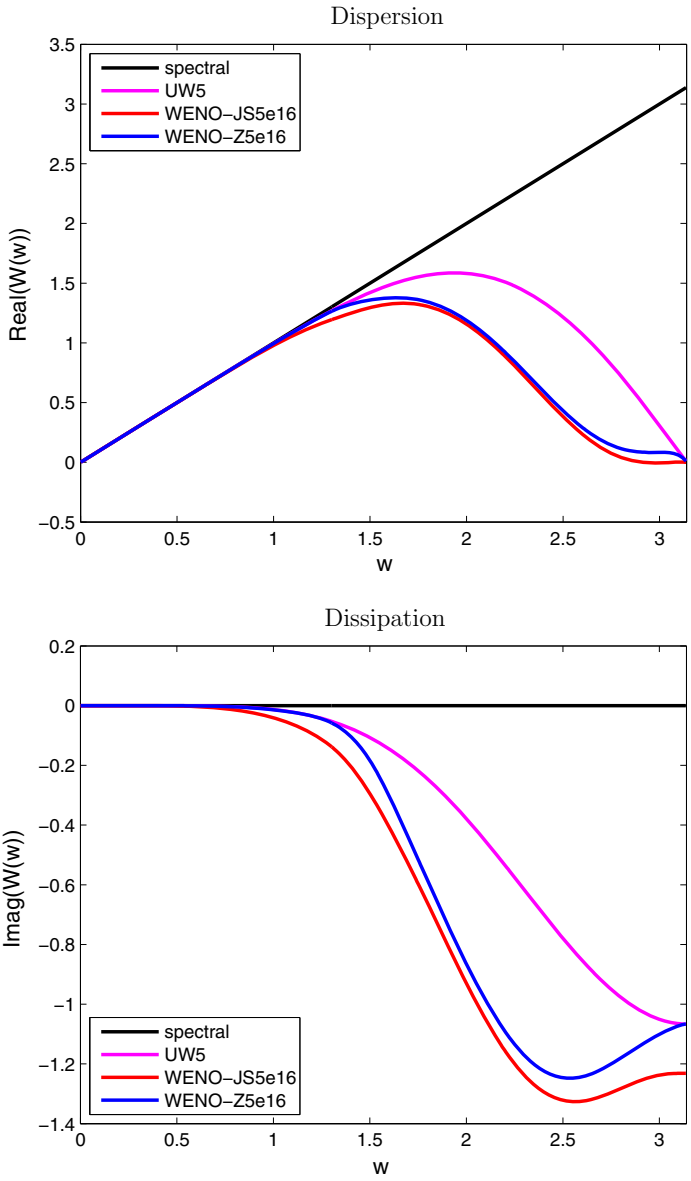

Fig. 2 (Color online) The spectral properties of the UW5 scheme, the WENO-JS5e16 scheme, and the WENO-Z5e16 scheme as analyzed by the approximate dispersion relation

essentially the same but the WENO-JS scheme (red square and circle symbols) decays in a much faster rate than the other two schemes. At the high wavenumber $\omega = \pi/2$, the WENO schemes (blue and red cross symbols) decay faster than the UW scheme (purple solid line). Overall, the WENO-Z scheme is less dissipative than the WENO-JS scheme and its spectral properties closely resemble the one of the UW scheme in the low-medium range wavenumbers.

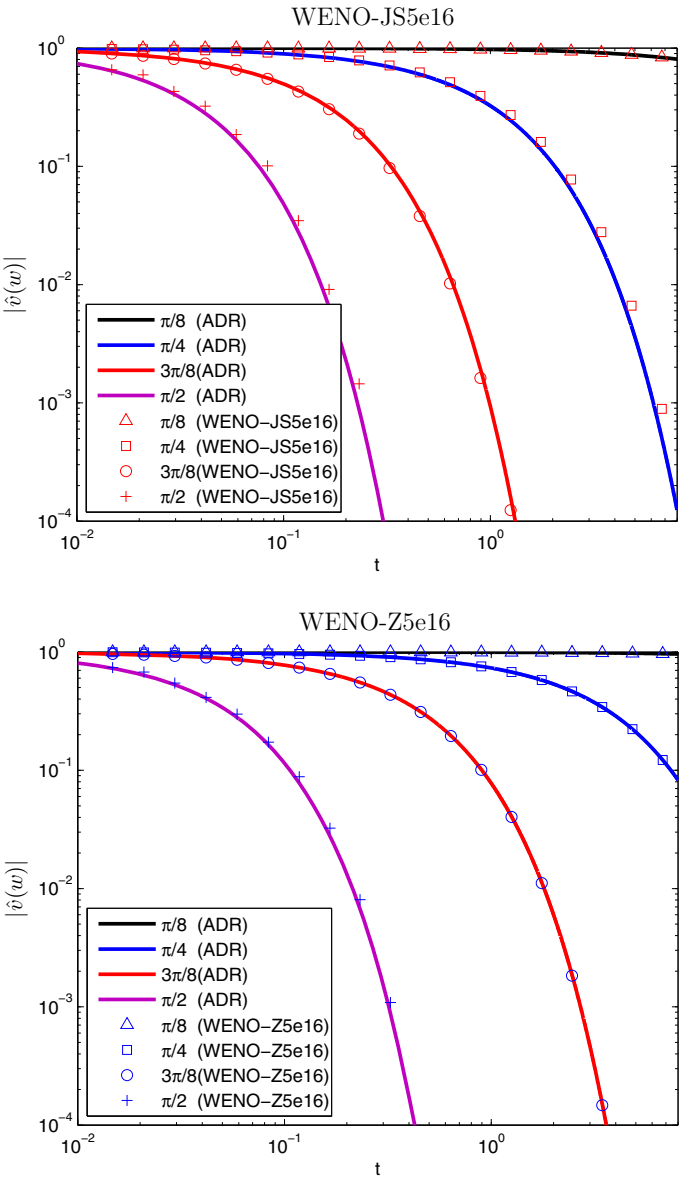

Fig. 3 (Color online) Temporal evolution of amplitude of Fourier modes $\omega = \pi/8, \pi/4, 3\pi/8$ and $\pi/2$ computed by the WENO-JS5e16 scheme and the WENO-Z5e16 scheme

3.2 ADR for an Initial Broadband Wave

Next, we consider the solution of the linear advection equation with an initial condition containing a broad range of wavenumbers [13],

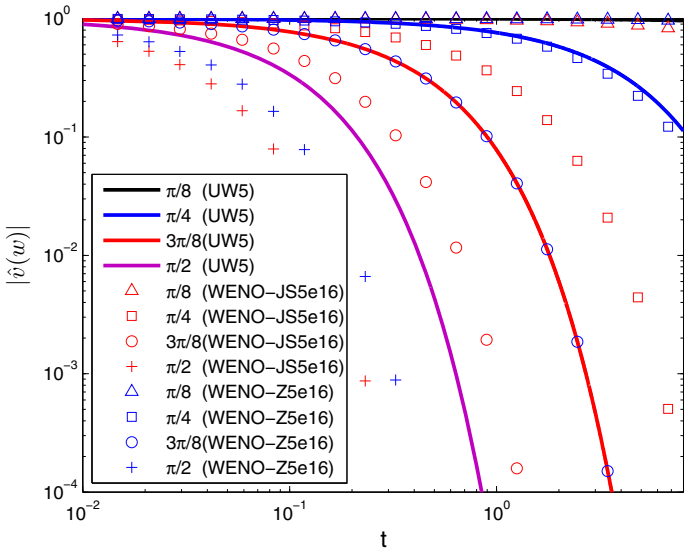

Fig. 4 (Color online) Temporal evolution of the amplitude of the spectrum of the the UW5 scheme, the WENO-JS5e16 scheme, and the WENO-Z5e16 scheme with an initial condition $v(x,0) = e^{i\kappa x}$, where $\omega = \pi/8, \pi/4, 3\pi/8$, and $\pi/2$

$$v_j(0) = \sum_{m=1}^{N/2} e^{-(\omega_m/(\pi/8))^2} e^{i(j\omega_m+\theta_m)}, \tag{19}$$

where ω_m are some assigned wavenumbers and θ_m are random phases.

In this case, we run the simulation with the third order Runge-Kutta TVD scheme for a long time and set the final time $t = 8$. Also, the sensitivity parameter ϵ plays an important role in the behavior of the spectral properties of the nonlinear schemes. Here, we use $\epsilon = 10^{-6}$ and $\epsilon = 10^{-16}$.

In Figs. 5 and 6, we show the amplitude spectra computed by the WENO schemes with $\epsilon = 10^{-6}$ and $\epsilon = 10^{-16}$, respectively. Each figure includes the amplitude spectra of the exact solution (solid black line), the theoretical prediction by the ADR (solid lines except the black line) and the numerical prediction (symbols) computed by the UW scheme, the WENO-JS scheme, and the WENO-Z scheme. The results agree well with those in [13]. As a linear scheme, the amplitude spectrum computed by the UW scheme (purple symbols) agrees well with the theoretical prediction (purple solid line). More important, the linear scheme does not generate *spurious* high modes. On the other hand, the amplitude spectra computed by the WENO-JS scheme (red square symbols) and the WENO-Z scheme (blue square symbols) only agree well with the theoretical prediction (red and blue solid lines) for wavenumbers $|\omega| < \omega_s$, a critical wavenumber.

Moreover, the agreement of the theoretical and numerical predictions depend on the value of the ϵ. In the case of $\epsilon = 10^{-6}$, the critical wavenumbers are $\omega_s = 0.45$ and $\omega_s = 0.8$ for the WENO-JS scheme and the WENO-Z scheme, respectively. Also, as expected, the amplitude spectrum computed by the WENO-JS scheme (red symbols) shows the scheme is far more dissipative than that of the UW scheme (purple symbols), while the amplitude spectrum computed by the WENO-Z scheme (blue symbols) is almost identical to that of the UW scheme up to the critical wavenumber $\omega_s = 0.8$. Both nonlinear schemes exhibit

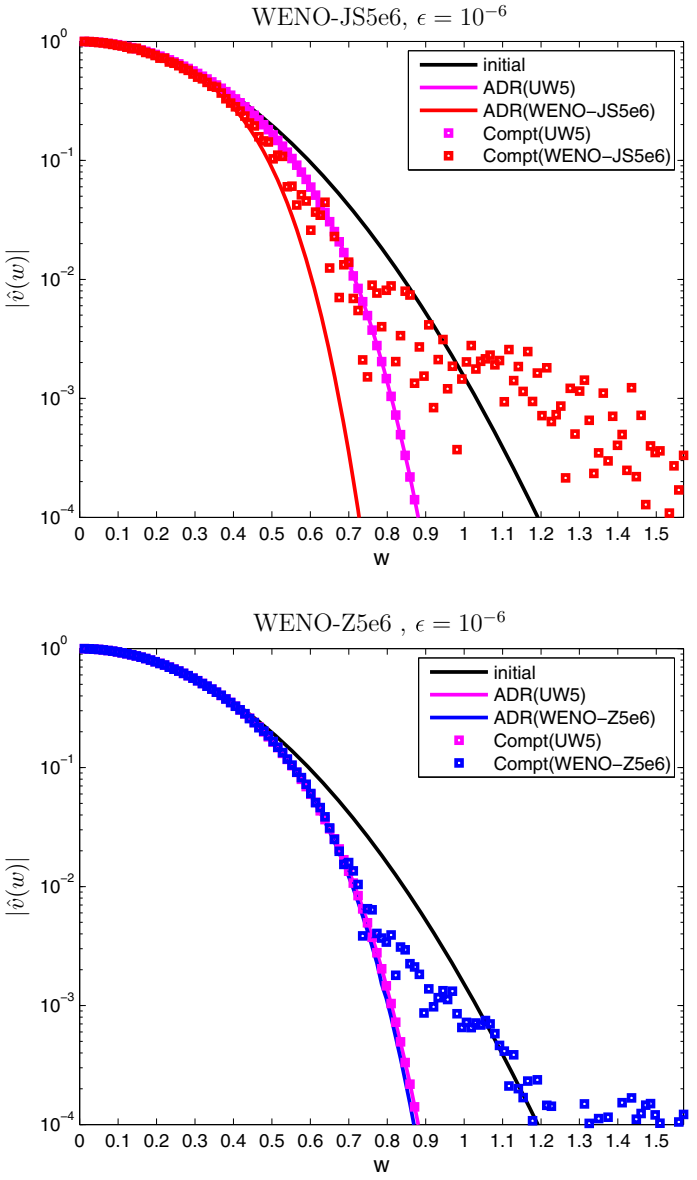

Fig. 5 (Color online) Amplitude spectra predicted by the ADR (*solid lines*) and computed by the UW5 scheme, the WENO-JS5e6 scheme, and the WENO-Z5e6 scheme (*symbols*) with an initial broadband wave at $t = 8$

spurious high modes in which the amplitudes of the high modes computed by the WENO-JS scheme is larger by a factor of ten than those computed by the WENO-Z scheme.

Similar observation can be made in the case of $\epsilon = 10^{-16}$ where the critical wavenumbers are $\omega_s = 0.4$ and $\omega_s = 0.55$ for the WENO-JS scheme and the WENO-Z scheme, respectively. However, the amplitude of the spurious high modes of both WENO schemes are larger and of the same order.

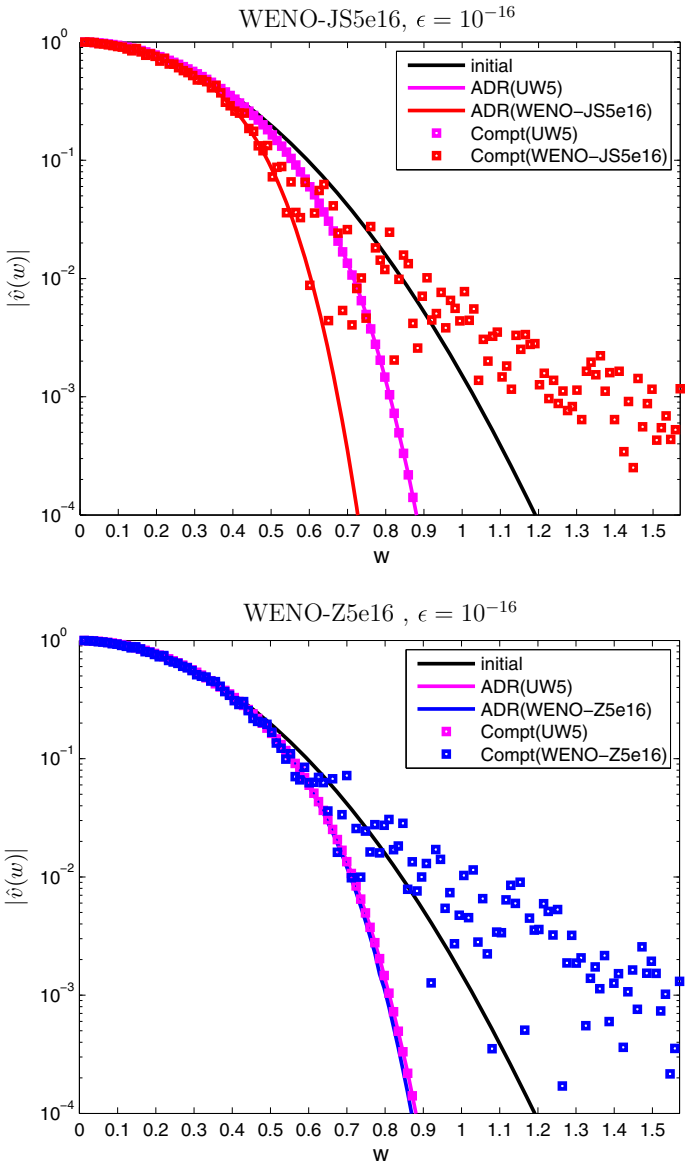

Fig. 6 (Color online) Amplitude spectra predicted by the ADR (*solid lines*) and computed by the UW5 scheme, the WENO-JS5e16 scheme, and the WENO-Z5e16 scheme (*symbols*) with an initial broadband wave at $t = 8$

We should remark that the amplitude of the spurious high modes is larger with a smaller ϵ, which controls the nonlinear stencils adaptation of the nonlinear schemes. That is, the more sensitive the nonlinear stencils adaptation (smaller ϵ) is, the smaller the critical wavenumber ω_s and the larger the amplitudes of the spurious high modes generated by the nonlinear schemes will be. The spurious high modes are inherent in the nonlinear schemes. Hence, for smooth flows, it is preferable to use a large ϵ if possible for a reduction but not total removal of spurious high modes when using the nonlinear schemes.

Remark 6 While the ADR has a very good capability to predict the spectral properties of the nonlinear schemes, it has some limitations.

1. Firstly, it only considers the evolution of a single wavenumber at a time but not a solution containing an entire spectrum of scales.
2. Secondly, it does not account for potential adverse effects of a long time integration.
3. Thirdly, it ignores the generation and nonlinear interactions of the spurious high modes by the nonlinear schemes, and their nonlinear impact on the evolution of a transported field [6].

For example, some turbulence flows, containing both low and high wavenumbers with a kinetic energy spectrum decay at a certain rate as a log of an increasing wavenumber, though looks chaotic, do not contain any true singularity (discontinuity/shock).

This leads us to examine the spectral properties of the nonlinear schemes via the nonlinear spectral analysis (NSA) as described in the next section.

4 Nonlinear Spectral Analysis

In this section, we will briefly describe the nonlinear spectral analysis (NSA) (see [7] for details). Similar to the ADR, the NSA solves a linear advection equation by a numerical scheme at limit of time $t = \Delta t \to 0$. The use of the linear advection problem, which serves as the fundamental model for complex hyperbolic systems, gives the exact analytical solution for assessing the basic performance of a numerical scheme. The main difference between the ADR and the NSA is the setup of the initial condition. In the NSA, the initial condition employs a more realistic broadband wave spectrum that contains not only large scale structures but also many smooth and small scale structures often found in a more realistic physical problem. The broadband wave consists of all resolvable wavenumbers with a predefined energy spectrum of the Fourier wavenumbers $E \propto \omega^{\alpha}$ and a uniformly distributed random phases, likes one might find in isotropic turbulence, in a 2π-periodical domain.

In this study, the energy spectrum of an initial synthetic field $u(x)$ in the Fourier space is

$$E(\omega) \propto \begin{cases} \omega^{\alpha}, & 0 < \omega \leq \omega_d \\ 0, & \omega_d < \omega \leq \pi \end{cases}, \tag{20}$$

where ω_d is a user defined cutoff mode and the maximum resolvable wavenumber is $\omega_{max} = \pi$.

The phase $\theta(\omega)$ of each Fourier mode is chosen randomly according to a uniform distribution $\mathcal{U}[-\pi, \pi]$, that is,

$$\theta(\omega) = \begin{cases} \mathcal{U}[-\pi, \pi], & 0 < \omega \leq \omega_d \\ 0, & \omega_d < \omega \leq \pi \end{cases}. \tag{21}$$

By taking the Fourier transform of $u(x)$, one has

$$\hat{u}(\omega) = \mathcal{F}\{u(x)\} = a(\omega) + ib(\omega), \tag{22}$$

and, equivalently,

$$\hat{u}(\omega) = \begin{cases} \pm\sqrt{U_0}\omega^{\frac{\alpha}{2}} \frac{1+i\tan(\theta(\omega))}{\sqrt{1+\tan^2(\theta(\omega))}}, & 0 < \omega \leq \omega_d \\ 0, & \omega_d < \omega \leq \pi \end{cases}, \tag{23}$$

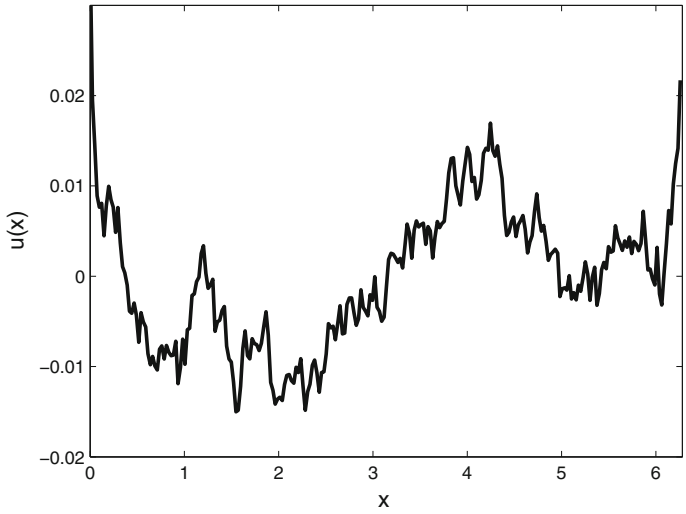

Fig. 7 The broadband wave function $u(x)$ in the physical space

with a random phase

$$\theta(\omega) = \arctan\left(\frac{b(\omega)}{a(\omega)}\right), \quad 0 < \omega \le \omega_d. \tag{24}$$

Therefore, the predefined energy spectrum (20) can be redefined as

$$E(\omega) = a(\omega)^2 + b(\omega)^2 = U_0\omega^\alpha, \quad 0 < |\omega| \le \omega_d, \tag{25}$$

where U_0 is a proportionality factor and set to be $U_0 = 1$ for the following discussion. To set the mean of $u(x) = 0$, we impose the condition that $E(\omega = 0) = 0$.

By taking the inverse Fourier transform, one readily obtains the synthetic field in the physical space $u(x)$ (see Fig. 7) in which the derivative $\frac{du}{dx}$ is discretized by a linear or nonlinear finite difference scheme. The modified wavenumber $W(\omega)$ of the discretized differentiation operator can then be determined as

$$W(\omega) = -\frac{i}{\hat{u}(\omega)}\mathcal{F}\left\{\frac{du}{dx}\right\}, \quad |\omega| \le \omega_d. \tag{26}$$

The analytical expression of the modified wavenumber can be easily derived for a linear scheme but not for a nonlinear scheme. Hence, (26) is considered as a good and workable alternative to estimate the spectral properties of a nonlinear scheme. In this scenario, the phase function $\theta(\omega)$ in (23) should be considered as the k-th random realization (sample) $\theta_k(\omega)$ of a uniform distribution of the phases in the interval $[-\pi, \pi]$. Hence, the modified wavenumber $W(\omega, \theta_k)$ depends on that particular realization $\theta_k(\omega)$ of the phase $\theta(\omega)$. With sufficient samples (random phases), we shall examine the statistics of the modified wavenumbers $W(\omega, \theta_k)$. In particular, we are interested in the expectation (mean) $\overline{W}(\omega) = \mathrm{E}(W(\omega, \theta_k))$ and the corrected sample standard deviation $\sigma_W(\omega) = \sqrt{\mathrm{Var}(W(\omega, \theta_k))}$, that is,

$$\overline{W}(\omega) = \frac{1}{M}\sum_{k=1}^{M} W(\omega, \theta_k), \qquad \sigma_W(\omega) = \left\{\frac{1}{M-1}\sum_{k=1}^{M}\left[W(\omega, \theta_k) - \overline{W}(\omega)\right]^2\right\}^{\frac{1}{2}}, \tag{27}$$

where M is the number of samples.

Furthermore, the energetic impact of the nonlinear mechanism is investigated. The dissipation effect on and the behavior of spurious high modes in the energy spectrum are also studied [9,13]. In analogy with the analytical relationship

$$\widehat{\frac{\partial u}{\partial x}} = i\omega\hat{u}, \tag{28}$$

one can define a reconstructed synthetic field $u_r(x)$ as

$$\widehat{\frac{\partial u_r}{\partial x}} = i\omega\hat{u}_r. \tag{29}$$

Then the energy spectrum of the reconstructed field can be obtained as

$$E_r(\omega,\theta_k) = \tfrac{1}{\omega^2}E_{\frac{\partial u}{\partial x}}(\omega,\theta_k) = \begin{cases} \frac{W^2}{\omega^2}E(\omega,\theta_k), & 0<\omega\le\omega_d, \\ \text{spurious modes}, & \omega_d<\omega\le\pi. \end{cases}. \tag{30}$$

In analogy with the synthetic field $u(x)$, one can obtain the statistics of the derivative of the synthetic field, $u_r(x)$. Moreover, we can easily obtain the expectation $\overline{E}_r(\omega) = \mathrm{E}(E_r(\omega,\theta_k))$ and the corrected sample standard deviation $\sigma_{E_r}(\omega) = \sqrt{\mathrm{Var}(E_r(\omega,\theta_k))}$ as well (see [6,7] for details).

4.1 Analysis of the Modified Wavenumber

In the following numerical examples, we consider the turbulent energy spectrum with decay rate $\alpha = -5/3$ and a cutoff wavenumber $\omega_d = \pi$. In some cases, we also consider setting the cutoff wavenumbers $\omega_d = \frac{2}{3}\pi$ and $\omega_d = \frac{1}{2}\pi$, to remove the aliasing error [12]. The statistical information is extracted from $M = 10^4$ samples of the synthetic field $u(x)$. The number of grid points $N = 256$, 512, 1,024 and 2,048 have been used to generate the statistics of the field. The results are very similar in nature and the general behaviors do not deviate much from each other in any discernible manner.

In Fig. 8, the statistics of the spectral properties of the WENO schemes with $\epsilon = 10^{-16}$, which agree well with those in [6], are shown. We have also tested the problem with $\epsilon = 10^{-6}$ and $\epsilon = 10^{-10}$. Since the solution, with sufficient resolution, is relatively smooth, their spectral properties are similar to those computed with $\epsilon = 10^{-16}$, and hence, they are omitted here. We observe that, for different random phases, the spectral properties of the WENO schemes are different; and, as expected, it has no effect on the spectral properties of the UW scheme. Although the spectral properties of the WENO schemes behave similarly, the WENO-Z scheme is always less dissipative for all wavenumbers $|\omega| < \pi$.

Statistically speaking, the numerical dispersion could become negative for high wavenumbers $|\omega| > 0.55\pi$ and there exists a tiny probability (less than 2 %) of anti-dissipation for low wavenumbers $|\omega| < 0.5\pi$. The amplitude of waves with these low wavenumbers could possibly be slightly amplified instead of reduced. In Table 1, the maximum of the anti-dissipation for one, two and three standard deviations $\overline{W}(\omega) \pm k\sigma_W(\omega), k = 1, 2, 3$ and their corresponding wavenumbers for the nonlinear schemes are given. One can see that the maximum anti-dissipation of the WENO-Z scheme is less than that of the WENO-JS scheme. Hence, statistically speaking, the WENO-Z scheme is a relatively safer algorithm.

The standard deviations of dissipation computed by the WENO schemes are shown in Fig. 9. We observe that the standard deviation of the WENO-Z scheme is less than that of the WENO-JS scheme in the whole range of resolvable wavenumbers. This indicates that

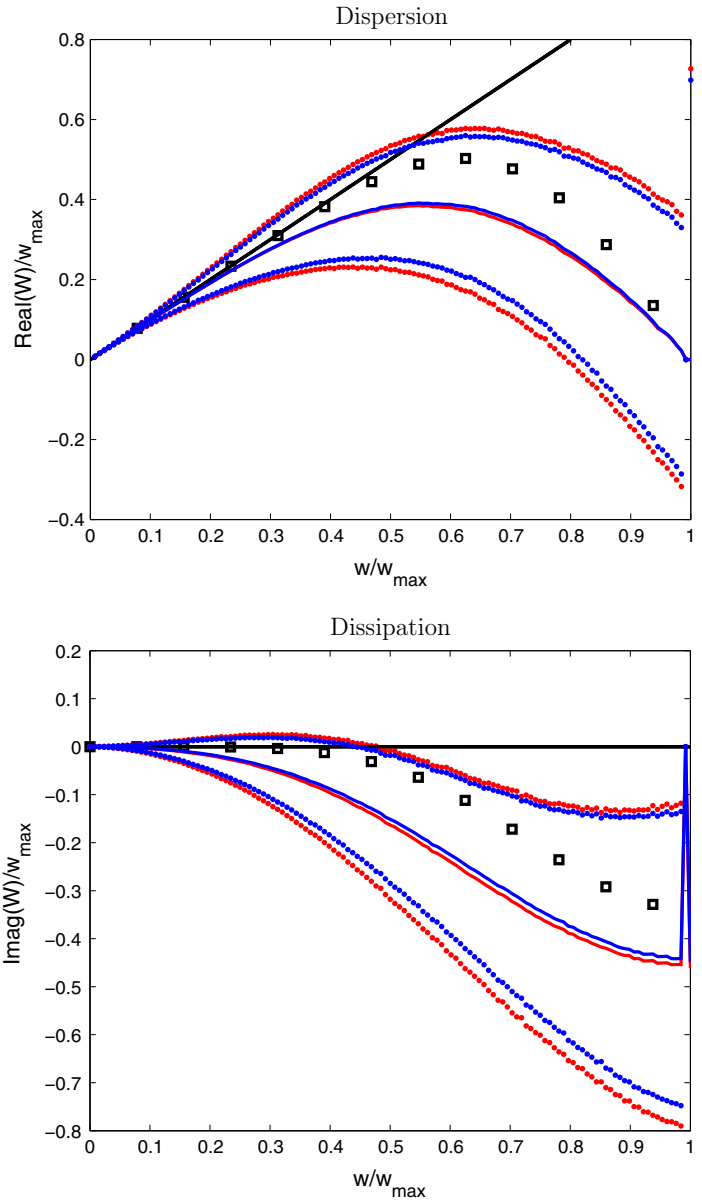

Fig. 8 (Color online) The spectral properties of the modified wavenumbers $W(\omega, \theta_k)$ (*solid line*) and $\overline{W}(\omega) \pm 2\sigma_W(\omega)$ (*dotted line*) for the WENO-JS5e16 scheme (*red line*) and the WENO-Z5e16 scheme (blue line) and the UW5 scheme (*black square*). The sensitivity parameter is $\epsilon = 10^{-16}$

the WENO-Z scheme is less sensitive to the random phases. It is important in simulating complex flow because random and erratic phases of flow usually appear. The less sensitivity of the WENO-Z scheme to the random phases would make a simulation more trustworthy.

Remark 7 The anti-dissipation only appears with a small probability in the NSA of the WENO nonlinear spatial differentiation operator with a broadband signal with random phases.

Table 1 Maximum anti-dissipation and its corresponding wavenumber with 1, 2 and 3 standard deviations of the WENO-JS scheme and the WENO-Z scheme

	$1\sigma_W(\omega)$		$2\sigma_W(\omega)$		$3\sigma_W(\omega)$	
	$\text{Imag}(W)_{max}$	ω	$\text{Imag}(W)_{max}$	ω	$\text{Imag}(W)_{max}$	ω
WENO-JS5	0.005	0.42	0.08	0.93	0.24	1.35
WENO-Z5	0.003	0.39	0.06	0.93	0.19	1.30

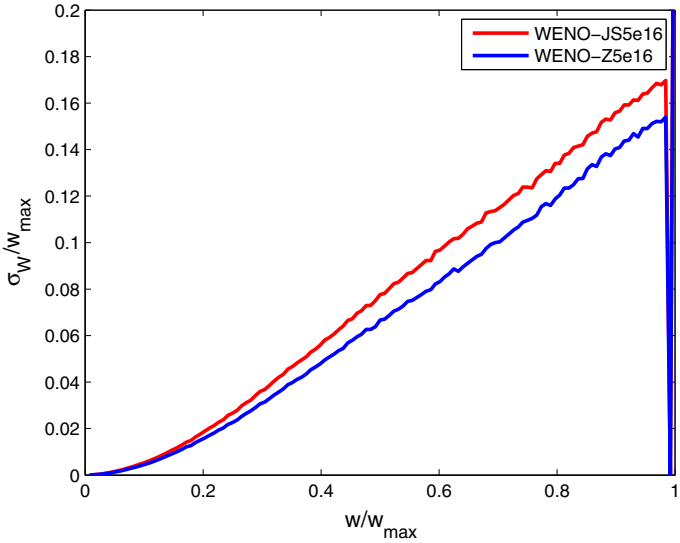

Fig. 9 (Color online) The standard deviations of dissipation computed by the WENO-JS5 scheme and the WENO-Z5 scheme. The sensitivity parameter is $\epsilon = 10^{-16}$

The stability of the numerical scheme depends also on the time discretization scheme used as well. As proved and demonstrated in [16] that the Euler forward scheme and all second order Runge-Kutta schemes are unstable for the WENO-JS5 scheme. They solved the linear advection equation with the WENO-JS5 scheme with an initial simple smooth sine function, and the resulting algorithm was unstable. The third and higher order strong stability preserving Runge-Kutta scheme (SSP) schemes, on the other hands, are stable with a stable CFL number. There are additional dissipation mechanisms such as the lower order dissipative Lax-Friedrichs flux splitting and limiters that will also help in stabilizing the WENO schemes.

4.2 Analysis of the Energy Spectrum

Here, we investigate the impact of the nonlinearity on the energy spectrum of the synthetic field, which is represented by the energy spectrum of the reconstructed field in (30). The cutoff wavenumber is chosen as $\omega_d = \pi/2$. The analytical energy spectrum and those computed by the UW scheme, the WENO-JS scheme, and the WENO-Z scheme with $\epsilon = 10^{-6}$ and $\epsilon = 10^{-16}$ is shown in Fig. 10. The results agree well with those given in [6]. The results with $\epsilon = 10^{-10}$ are almost identical to those with $\epsilon = 10^{-16}$, and they are omitted here.

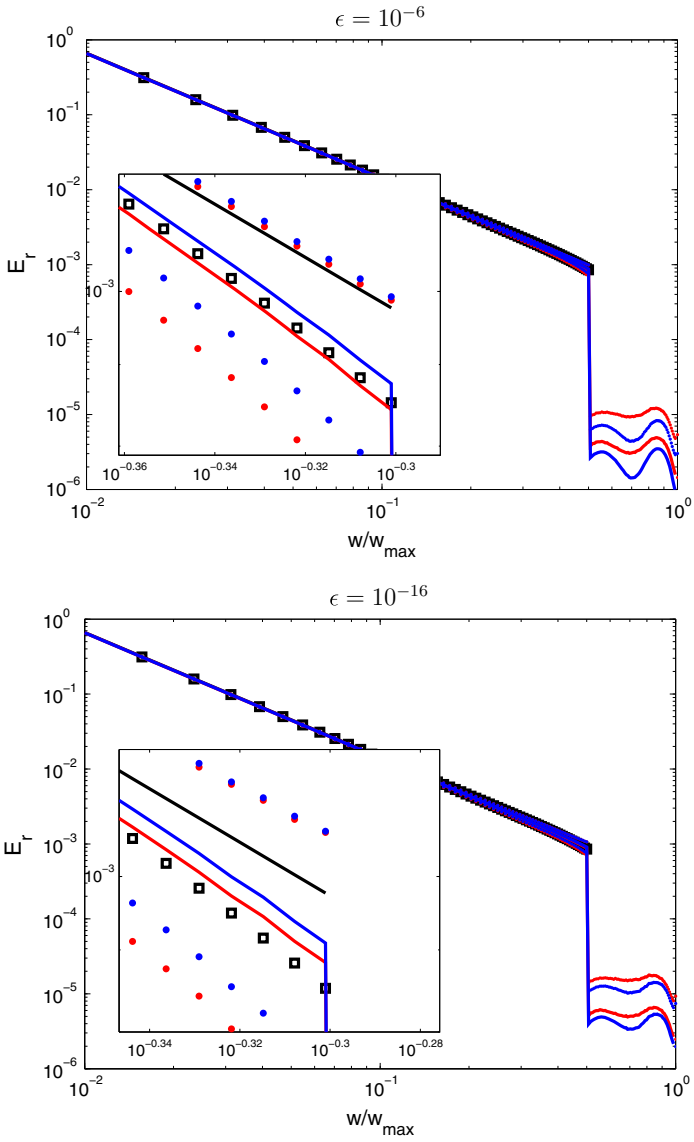

Fig. 10 (Color online) The spectra of the mean energy field $\overline{E}_r(\omega)$ and its two standard deviations from the mean $\overline{E}_r(\omega) \pm 2\sigma_{E_r}(\omega)$ as computed by the UW5 scheme (*black square*), the WENO-JS5 scheme (*red solid/dotted line*) and the WENO-Z5 scheme (*blue solid/dotted line*). The *solid black line* is the energy spectrum of the exact solution. The cutoff wavenumber is $\omega_d = \pi/2$. The sensitivity parameters are $\epsilon = 10^{-6}$ and $\epsilon = 10^{-16}$

In the case of $|\omega| \leq \omega_d$, the energy spectra agrees well with the analytical energy spectrum, which indicates that all three schemes conserve the energy of the system very well. Compared with the analytical energy spectrum, the slightly decreased energy spectra can be observed in the zoomed figures. We also observe that the WENO-Z scheme usually loses the least energy and the UW scheme and the WENO-JS scheme lose the most energy for $\epsilon = 10^{-16}$ and $\epsilon = 10^{-6}$, respectively.

With the decreases of the sensitivity parameter ϵ, the energy spectra computed by the WENO schemes are closer to the analytical one. The energy spectrum computed by the WENO-Z scheme is always closer to the analytical energy spectrum than those computed by the UW scheme and the WENO-JS scheme. In this case, the spurious modes, with wavenumber $|\omega| > \omega_d$, are generated by the WENO schemes, which have been reported in [5,6,9]. These spurious modes interact nonlinearly with all other modes and might have a severe impact on the evolution of the solution of a nonlinear equation. Obviously, the spurious modes generated by the WENO-Z scheme are less than those generated by the WENO-JS scheme. These results indicate that, compared with the WENO-JS scheme, the WENO-Z scheme is better at preserving energy and generating less spurious modes intrinsically.

4.3 Propagation of a Broadband Wave

Next, we examine the behavior of the WENO schemes in the context of long-time integration based on an elementary numerical experiment [7]. We consider the linear advection equation (1) with a constant velocity $v = \pi$ which transports a broadband signal (23) through a periodic domain. The cutoff wavenumber is $\omega_d = 2/3\pi$. The standard six-stages low-storage Runge Kutta method [6] is used for the time integration. The number of grid points is $N = 1024$ and the time step is $\Delta t = 10^{-6}$. The relative error on the energy spectrum $\Delta E(w, t)$ and the energy spectrum of the error $E_\Delta(w, t)$, are defined as

$$\Delta E(w,t) = \frac{\Delta(|\hat{u}|^2)}{\gamma}, \quad E_\Delta(w,t) = \frac{|\Delta(\hat{u})|^2}{\gamma}, \tag{31}$$

where $\gamma = \int_{-\pi}^{\pi} |\hat{u}|^2 d\omega$, $\Delta f \equiv f - f_n$, $|f| = \sqrt{ff^*}$, and u and u_n are the exact and numerical solutions respectively.

In Figs. 11 and 12, we show the spectra of the energy of the field $\Delta E(\omega, t)$ and $E_\Delta(\omega, t)$ as computed by the UW scheme and the WENO schemes at time $t = 2$. The results agree well with those given in [7]. In the case of $|\omega| \leq \omega_d$, the two error measurements $\Delta E(\omega, t)$ and $E_\Delta(\omega, t)$ computed by the WENO-Z scheme are sandwiched between the ones computed by the WENO-JS scheme and the UW scheme. For the cutoff wavenumber $\omega_d \leq \pi$, the WENO schemes generate spurious high modes which may pollute the solution. For $\epsilon = 10^{-6}$, the spurious energy is very small, lower than the energy at $|\omega| = \omega_d$ about 10 order of magnitudes. Also, the spurious energy is produced less by the WENO-Z scheme. For $\epsilon = 10^{-16}$, the energy of spurious modes generated by the WENO-Z scheme slightly larger. It is due to the larger dissipation of the WENO-JS scheme in high wavenumbers, which reduces the generation of spurious high wavenumbers during the time evolution. In either cases, the spurious energy is still very small in an order of $O(10^{-10})$. In summary, the WENO-Z scheme preserves the energy spectrum better than the WENO-JS scheme in a long time simulation.

4.4 Energy Spectra of Solution with Discontinuities

Since the WENO schemes are ultimately designed to handle hyperbolic PDEs with a discontinuous solution, a more interesting linear advection problem with a square wave is considered here. In this simple example, the third order Runge-Kutta-TVD method is used for the time integration. The number of grid points is $N = 300$ and the time step is $\Delta t = 10^{-3}$. The numerical solutions and energy spectra computed by the UW scheme, the WENO-JS scheme, and the WENO-Z scheme with the sensitivity parameter $\epsilon = 10^{-16}$ are shown in Fig. 13. The oscillations around the two discontinuities are observed for the UW scheme but not for the WENO schemes, which avoid performing interpolation across the discontinuities by the

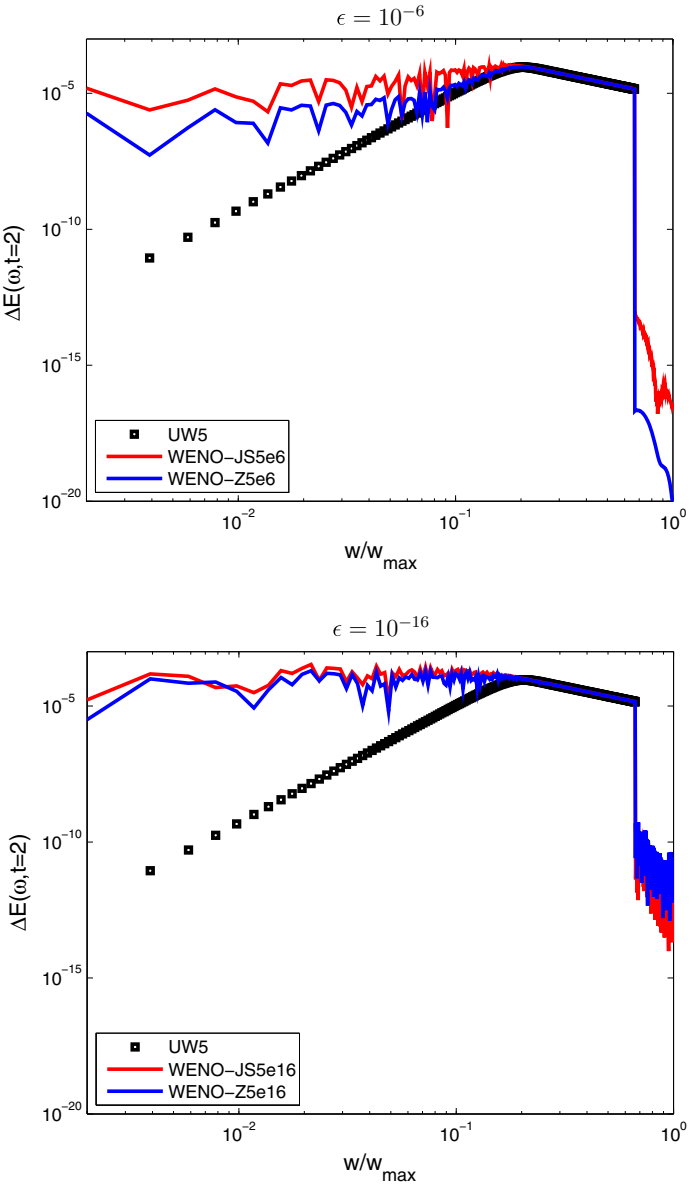

Fig. 11 (Color online) The relative error of the energy spectrum $\Delta E(\omega, t = 2)$ in solving the linear advection equation with a broadband wave as computed by the UW5 scheme (*black square*), the WENO-JS5 scheme (*red solid line*) and the WENO-Z5 scheme (*blue solid line*). The cutoff wavenumber is $\omega_d = 2\pi/3$. The sensitivity parameters are $\epsilon = 10^{-6}$ and $\epsilon = 10^{-16}$

nonlinear stencils adaptation. From the zoomed figures, the WENO-Z scheme is slightly less dissipative than the WENO-JS scheme at the discontinuities. The numerical and analytical energy spectra agree well with each other for wavenumbers $|w| \leq 0.08\pi$, and the energy spectra decreases with the increase of the wavenumbers. At the higher wavenumbers, the UW scheme loses the most energy while the WENO-Z scheme loses the least energy. Fur-

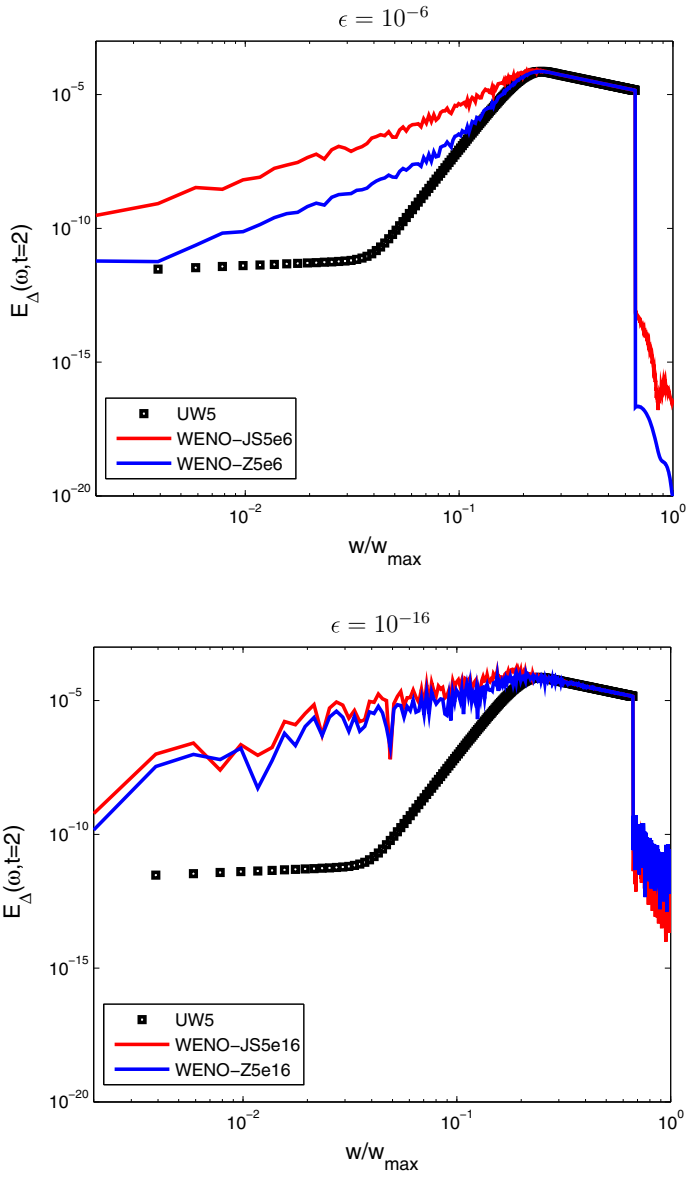

Fig. 12 (Color online) The energy spectrum of the error $E_\Delta(\omega, t = 2)$ in solving the linear advection equation with a broadband wave as computed by the UW5 scheme (*black square*), the WENO-JS5 scheme (*red solid line*) and the WENO-Z5 scheme (*blue solid line*). The cutoff wavenumber is $\omega_d = 2\pi/3$. The sensitivity parameters are $\epsilon = 10^{-6}$ and $\epsilon = 10^{-16}$

thermore, as shown in Fig. 14, $\Delta E(w, t)$ and $E_\Delta(w, t)$ computed by the UW scheme and the WENO schemes illustrate the fact that the oscillatory phenomena is due to the existence of discontinuous solution. The results with $\epsilon = 10^{-6}$ and $\epsilon = 10^{-10}$ are omitted here since they show essentially the same behavior as those in Figs. 13 and 14.

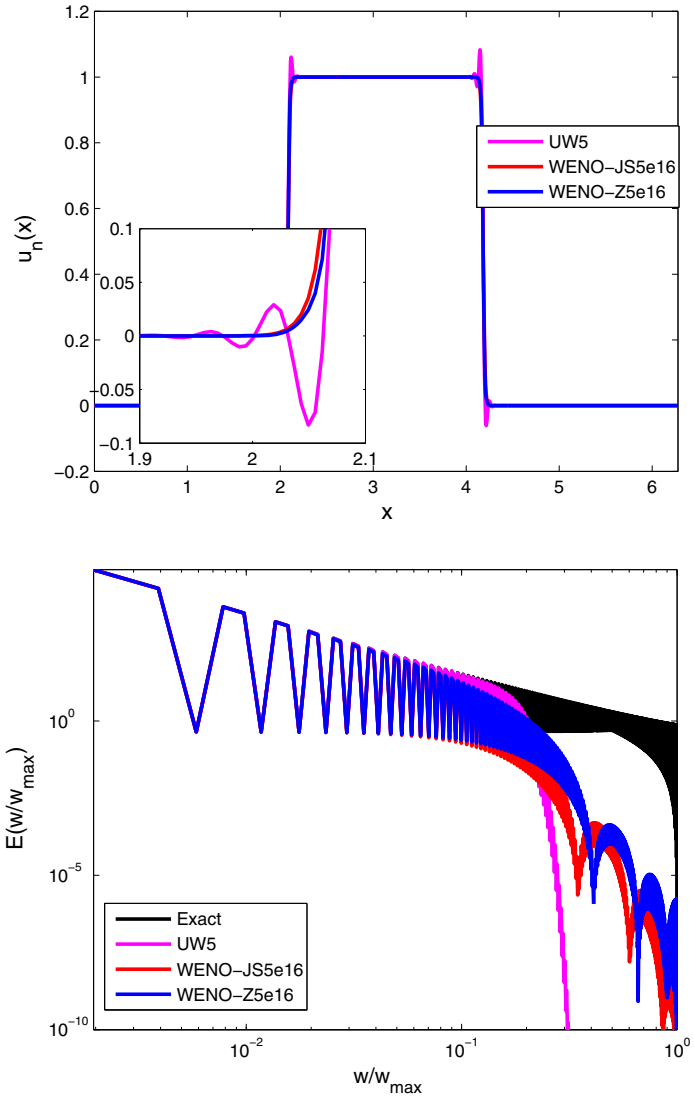

Fig. 13 (Color online) (*Top*) The numerical solution and (*Bottom*) the relative error of the energy spectrum in solving the linear advection equation with an initial square wave as computed by the UW5 scheme, the WENO-JS5 scheme and the WENO-Z5 scheme. The sensitivity parameter is $\epsilon = 10^{-16}$

5 ϵ-Adaptive WENO-Z Scheme

As we have observed in the previous discussion, the ϵ of the WENO schemes plays an important role in the development of nonlinear effects in an otherwise linear problem. To quantify the influence of the nonlinear stencils adaptation of the WENO schemes for different ϵ, we define a critical wavenumber ω_c for the dissipation and dispersion as

$$\omega_c^{\text{disp}} = \max\{\omega| \quad |\Re(W^{WENO} - W^{UW})| < \delta\},$$
$$\omega_c^{\text{diss}} = \max\{\omega| \quad |\Im(W^{WENO} - W^{UW})| < \delta\},$$

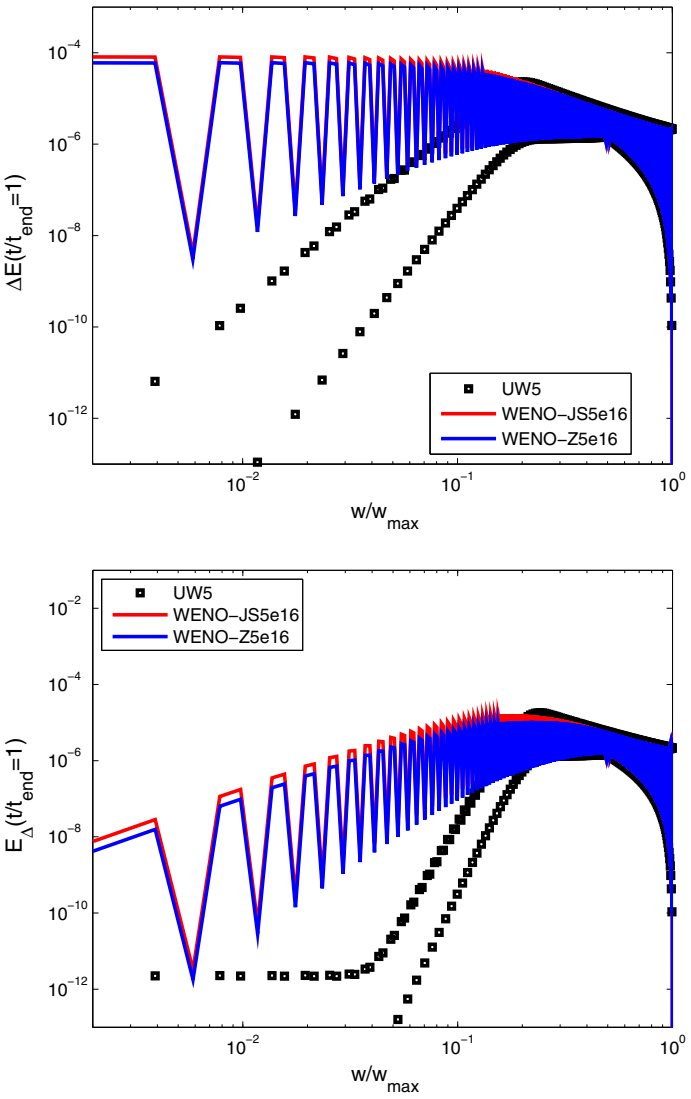

Fig. 14 (Color online) (*Top*) The relative error of energy spectrum $\Delta E(\omega, t = 2)$ and (*Bottom*) the energy spectrum of the error $E_\Delta(\omega, t = 2)$ in solving the linear advection equation with an initial square wave as computed by the UW5 scheme, the WENO-JS5 scheme and the WENO-Z5 scheme. The sensitivity parameter is $\epsilon = 10^{-16}$

where $\delta = 0.05$ is used in this test. We shall find the critical wavenumber ω_c such that for any wavenumbers $|\omega| \leq \omega_c$, the difference of the dissipation (dispersion) of the nonlinear schemes and the linear scheme is larger (smaller) than the given tolerance δ, for different values of ϵ. The larger the ω_c is, the closer the behaviors of the nonlinear scheme will be like the linear scheme.

From Fig. 15, we see that the critical wavenumber ω_c is fairly constant for sufficiently small $\epsilon \leq O(1)$ for both the WENO-JS scheme and the WENO-Z schemes and rises rapidly to the

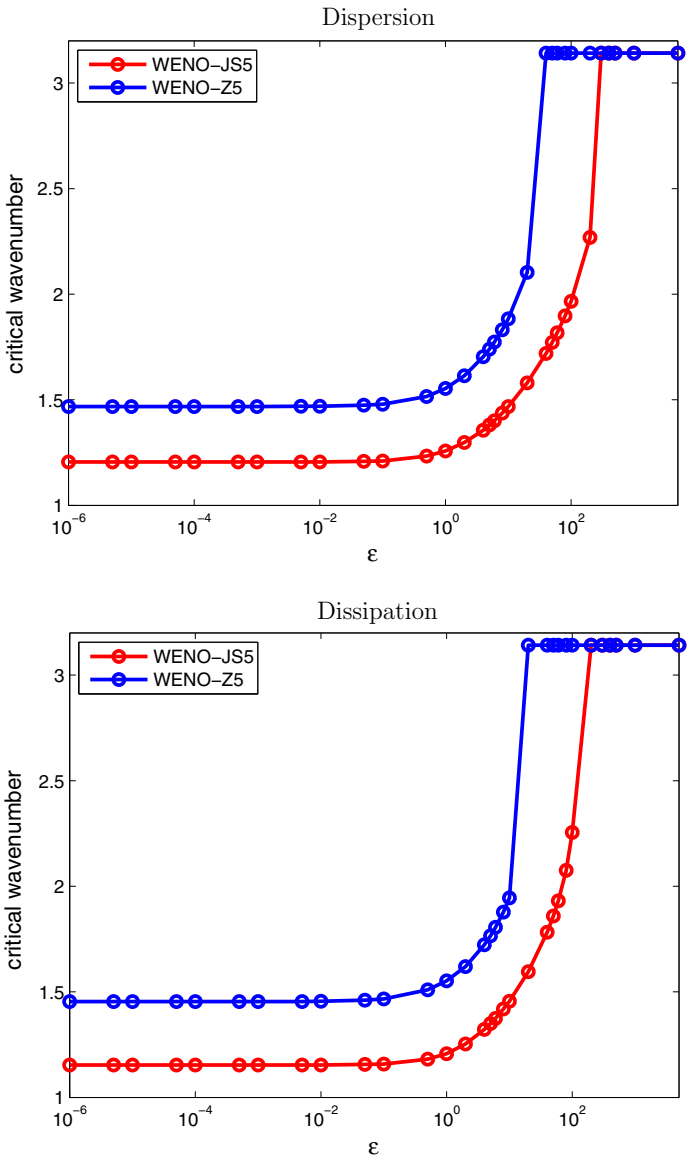

Fig. 15 (Color online) The critical wavenumber ω_c as a function of the sensitivity parameter ϵ with the WENO-JS5 scheme and the WENO-Z5 scheme

maximum value $\omega_c = \pi$. In term of dissipation, the figure shows that the WENO-JS scheme and the WENO-Z scheme have an asymptotic critical wavenumber of about $\omega_c \approx 1.2$ and $\omega_c \approx 1.45$, respectively. In other words, the WENO-Z scheme, as expected, is less dissipative than the WENO-JS scheme for all reasonable small ϵ. For $\epsilon > O(10)$ and $\epsilon > O(100)$, the WENO-Z scheme and the WENO-JS scheme, respectively, behave essentially the same as the linear scheme. This is expected as, for smooth solution, the sensitivity parameter ϵ will dominate over the local smoothness indicators β_k in the definition of the nonlinear weights

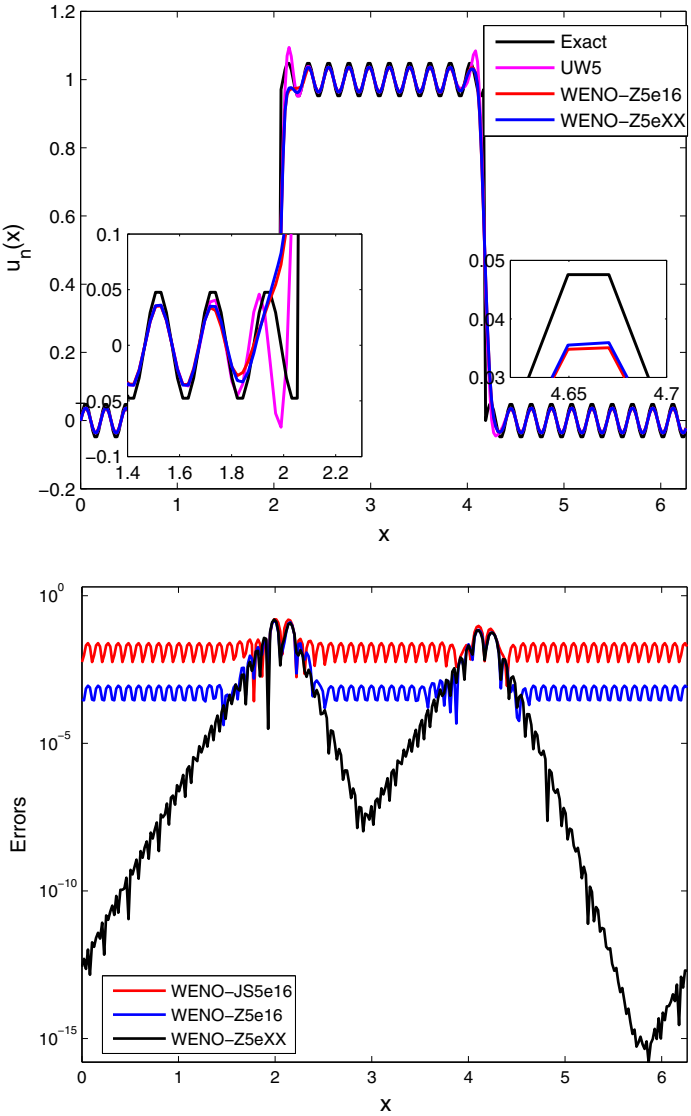

Fig. 16 (Color online) (*Top*) The advection of the square wave as computed by the UW5 scheme, the WENO-Z5e16 scheme and the WENO-Z5eXX scheme. (*Bottom*) The pointwise difference in absolute value between the UW scheme and the WENO schemes

ω_k [see (7) and (8)], and force them to almost equal to the ideal weights d_k with a difference between them in the order of $O(\epsilon^{-p})$ where p is the power parameter. Similar observations can be made from the dispersion relation.

An interesting observation can be deduced from the discussion above. If one could increase the sensitivity parameter ϵ according to the increased smoothness of the function, it is possible to achieve, in a smooth region, (1) the optimal order of the linear scheme, and (2) to reduce if not to avoid a number of numerical issues, such as the probability of small anti-dissipation

in the low wavenumber range and the generation of spurious high modes, associated with using a nonlinear scheme for an essentially smooth solution of the hyperbolic conservation laws.

We propose an ϵ-adaptivity technique that, instead of being a fixed small constant, the sensitivity parameter $\epsilon(x,t)$ is modified spatially and temporally according to the smoothness of the solution at a given spatial location and time, that is

$$\epsilon(x,t) = \begin{cases} \epsilon_{max}, & \text{if } \tau_5 \le S_{min} \\ \epsilon_{min}, & \text{if } \tau_5 \ge S_{max} \\ \exp(k_1 \ln(\tau_5) + k_2), & \text{if } S_{min} \le \tau_5 \le S_{max}, \end{cases} \tag{32}$$

where

$$k_1 = \frac{\epsilon_{max}/\epsilon_{min}}{\ln(S_{min}/S_{max})}, \quad k_2 = \ln(\epsilon_{max}) - k_1 \ln(\epsilon_{min}),$$

and τ_5 is the fifth order global smoothness indicator used in the WENO-Z5 scheme (8). Based on our experiences, we take the parameters $\epsilon_{min} = 10^{-16}$, $\epsilon_{max} = 10^{3}$, $S_{min} = 4 \times 10^{-4}$ and $S_{max} = 10^{-3}$ in this example. Other forms of (32) can be designed and it is a subject of a future research.

In the left figure of Fig. 16, we show the solutions computed by the UW5 scheme, the WENO-Z5e16 scheme, and the ϵ-adaptive WENO-Z5 scheme (WENO-Z5eXX). From the zoomed figures, we observe that the solution computed by the WENO-Z5eXX scheme is in a very good agreement with that computed by the WENO-Z5e16 scheme around the discontinuities and that computed by the UW5 scheme in the smooth part of the solution. To show the difference among the three WENO schemes, the absolute errors between the UW5 scheme and the WENO schemes are presented in the right figure of Fig. 16. It confirms the enhanced accuracy of solution with the ϵ-adaptive WENO-Z5 scheme in the smooth regions in this preliminary result.

6 Conclusion

In summary, we have applied the approximate dispersion relation (ADR) and the nonlinear spectral analysis (NSA) to the study of the dissipation and dispersion (spectral) properties of the nonlinear shock capturing schemes, in particular, the classical fifth order weighted essentially non-oscillatory finite difference scheme (WENO-JS5) and its improved version (WENO-Z5), when solving a linear advection equation with a periodical domain. We perform the spectral analysis on the WENO schemes while also taking into account of the influences of the sensitivity parameter ϵ found in the definition of the WENO nonlinear weights. As a benchmark, the fifth order upwinded central linear scheme (UW5) is used for the investigation of the performance of the nonlinear WENO schemes in terms of the spectral properties.

Firstly, we employ the ADR to predict theoretically the spectral behavior of four individual waves with a fixed wavenumber and compared that with the computed solution by the WENO schemes for a very short time. We find that the ADR is able to predict the spectral properties of the WENO differentiation operator quite reliably. The results also show that the WENO-Z5 scheme has a smaller dissipation and dispersion errors than the WENO-JS5 scheme. We also examine the nonlinear effects of the WENO schemes for a long time simulation of an initial broadband wave in which we find the generation of spurious high modes for both WENO schemes regardless of the value of ϵ. For $\epsilon = 10^{-6}$, the WENO-Z5 scheme has a better resolution power in the low to middle wavenumber ranges and amplitude of the

spurious high modes is ten times less than that of the WENO-JS5 scheme. For $\epsilon = 10^{-16}$, the amplitude of the spurious high modes generated by both WENO schemes are similar. The results indicate that the nonlinear stencils adaptation of the WENO schemes will generate spurious high modes of significant difference if the sensitivity parameter is chosen differently.

Secondly, due to the inherent limitations of the ADR, we also employed the NSA to investigate the statistical nonlinear behavior, due to nonlinear stencils adaptation of a WENO scheme, of the full spectra of the wavenumbers from a large set of synthetic scalar fields with a prescribed energy spectrum and random phases. The statistical results show that the WENO-Z5 scheme generates less dissipation and dispersion errors than the WENO-JS5 scheme in an entire wavenumber range, especially in the mid-wavenumber range. However, it is also interesting to find that the nonlinearity, statistically speaking, of both WENO schemes can generate a small amount of anti-dissipation in the low wavenumber range regardless of the value of ϵ. In this respect, the WENO-Z5 scheme generates slightly less anti-dissipation and in a lower probability than the WENO-JS scheme. Moreover, the standard deviations of both WENO schemes indicate that the WENO-Z5 scheme is less sensitive to random phases. It implies that the spectral behavior of the WENO-Z5 scheme is slightly more stable and accurate.

Finally, in light of the dependence between the spectral properties of the WENO schemes and the sensitivity parameter ϵ, we propose an ϵ-adaptivity technique in which the sensitivity parameter $\epsilon(x, t)$ is modified spatially and temporally according to the smoothness of the solution at a given spatial location and time. This would make it possible (1) to achieve, in a smooth region, the optimal order of the linear scheme, and (2) to reduce if not to avoid a number of numerical issues, such as the probability of anti-dissipation in the low wavenumber range and the generation of spurious high modes in the high wavenumber range, associated with the use of a WENO scheme for an essentially smooth solution of the hyperbolic conservation laws. The preliminary test of an advection of a square wave with the $\epsilon(x, t)$ shows that the solution is in a very good agreement with that computed by the WENO-Z5 scheme around the discontinuities and that computed by the UW5 scheme in the smooth part of the solution. The performance of the ϵ-adaptive WENO-Z5 scheme applied to more complex nonlinear problems will be investigated in the future work.

Acknowledgments The authors would like to express our sincere gratitude to Prof. Pirozzoli and Dr. Fauconnier for their valuable insights and comments during the course of this study. The authors would like to acknowledge the funding support of this research by China Postdoctoral Science Foundation (2012M521374, 2013T60684), Natural Science Foundation of Shandong Province (ZR2012AQ003), National Natural Science Foundation of China (11201441), Fundamental Research Funds for the Central Universities (201362033) and the startup funding by the Ocean University of China (Don). The authors (Don, Jia) would like to thank the School of Mathematical Sciences of Ocean University of China for hosting their visits in the First Summer Workshop in Advanced Research in Applied Mathematics and Scientific Computing 2013.

References

1. Balsara, D., Shu, C.W.: Monotonicity preserving weighted essentially non-oscillatory schemes with increasingly high order of accuracy. J. Comput. Phys. **160**, 405–452 (2000)
2. Borges, R., Carmona, M., Costa, B., Don, W.S.: An improved weighted essentially non-oscillatory scheme for hyperbolic conservation laws. J. Comput. Phys. **227**, 3191–3211 (2008)
3. Castro, M., Costa, B., Don, W.S.: High order weighted essentially non-oscillatory WENO-Z schemes for hyperbolic conservation laws. J. Comput. Phys. **230**, 1766–1792 (2011)
4. Don, W.S., Borges, R.: Accuracy of the weighted essentially non-oscillatory conservative finite difference schemes. J. Comput. Phys. **250**, 347–372 (2013)

5. Fauconnier, D., Langhe, C.D., Dick, E.: A family of dynamic finite difference schemes for large-eddy simulation. J. Comput. Phys. **228**(6), 1830–1861 (2009)
6. Fauconnier, D., Dick, E.: On the spectral and conservation properties of nonlinear discretization operators. J. Comput. Phys. **230**, 4488–4518 (2011)
7. Fauconnier, D., Dick, E.: Spectral analysis of nonlinear finite difference discretizations. J. Comput. Appl. Math. **246**, 113–121 (2013)
8. Jiang, G.S., Shu, C.W.: Efficient implementation of weighted ENO schemes. J. Comput. Phys. **126**, 202–228 (1996)
9. Ladeinde, F., Cai, X., Visbal, M.R., Gaitonde, D.V.: Turbulence spectra characteristics of high order schemes for direct and large eddy simulation. Appl. Numer. Math. **36**(4), 447–474 (2001)
10. Lele, S.K.: Compact finite-difference schemes with spectral-like resolution. J. Comput. Phys. **103**, 16–42 (1992)
11. Osher, S., Chakravarthy, S.R.: High resolution schemes and entropy conditions. SIAM J. Numer. Anal. **21**, 955–984 (1984)
12. Orszag, S.A.: On the elimination of aliasing in finite-difference schemes by filtering high-wavenumber components. J. Atmos. Sci. **28**, 1074 (1971)
13. Pirozzoli, S.: Short note: on the spectral properties of shock-capturing schemes. J. Comput. Phys. **219**(2), 489–497 (2006)
14. Shu, C.W.: High order weighted essentially nonoscillatory schemes for convection dominated problems. SIAM Rev. **51**(1), 82–126 (2009)
15. Vichnevetsky, R., Bowles, J.B.: Fourier Analysis of Numerical Approximations of Hyperbolic Equations. SIAM, Philadelphia (1982)
16. Wang, R., Spiteri, R.J.: Linear instability of the fifth-order WENO method. SIAM J. Numer. Anal. **45**(5), 1871–1901 (2007)